

Experimental Study of Surface Hardening of AISI 420 Martensitic Stainless Steel Using High Power Diode Laser

Mahmoud Moradi^{1,2} · Mohammad Meghdad Fallah³ · Saied Jamshidi Nasab^{1,2}

Received: 2 March 2018 / Accepted: 18 April 2018 / Published online: 16 May 2018
© The Indian Institute of Metals - IIM 2018

Abstract In this paper laser surface hardening of martensitic stainless steel AISI 420 was conducted using a 1600 W semiconductor diode laser. Focal plane position, laser power and scanning speed were considered as process variables. Microhardness was measured in depth and surface of the hardened layer and metallography of samples were conducted in order to study the microstructure of the hardened zone. Macrography was also performed to measure the geometrical dimensions of hardened zone (width and depth). Microstructure evaluation was investigated through optical microscopy and field emission scanning electron microscopy. Microstructure observation of laser treated zone indicated that the higher surface hardness created the finer and more uniform martensitic phase. Results showed that by increasing the laser power and decreasing the focal plane position, depth of penetration and microhardness of hardened zone increased. By increasing the scanning speed and focal plane position, penetration depth decreased while width of hardened zone increased. Under desired conditions resulting from this research (laser power 1400 W, scanning speed 5 mm/s and focal plane position 65 mm), surface hardness of AISI 420 martensitic steel increased to 720 from 210 Vickers. The dimension of hardened layer was 1.2 mm in depth and 6.1 mm in width. Comparing the results with the furnace hardening heat treatment showed that the laser

hardening process was more effective and precise than conventional processes.

Keywords Laser surface hardening · High power diode laser · Microhardness · Heat treatment · AISI 420 martensitic stainless steel

1 Introduction

There are common heat treatment methods for improving surface hardness of steels such as induced and flame heat treatment. The research trend is to improve the precision of the processes using modern technologies like laser surface treatment [1]. Recently laser material processing is used for several industrial applications such as laser welding and brazing [2–7], laser drilling [8], and laser cutting [9]. Diode high power laser which is commonly applied in industry can be used for high accuracy surface treatment of the parts.

Martensitic stainless steels are commonly used in manufacturing components employed specially in high stress and corrosion condition. These alloys are used in power plant and petrochemical industries as corrosion resistance components [10]. Steel grade 420 is a martensitic stainless steel that has corrosion resistance similar to 410 plus increased strength and hardness; so it is also used as turbo compressor blades in power plant industry. For increasing the surface hardness of the components, it is necessary to perform the process with selected laser parameters. These parameters are dependent on the laser source type, material specification and desired surface properties. While performing the process on martensitic steel parts, the surface hardness improves through transformation of the ferrite and austenite phases to martensitic

✉ Mahmoud Moradi
moradi.malayeru@gmail.com

¹ Department of Mechanical Engineering, Faculty of Engineering, Malayer University, Malayer, Iran

² Laser Materials Processing Research Center, Malayer University, Malayer, Iran

³ Shahid Rajaee Teacher Training University, P. O. Box: 16785-163, Lavizan, Tehran, Iran

phase in near surface of the part [11]. In the literature, there are several studies for achieving the proper input parameter of surface laser hardening process for different materials. Mahmoudi et al. [12] studied the surface hardening of AISI 420 using pulsed Nd:YAG laser and geometry of hardened layer was investigated. Also the corrosion resistance of this steel after laser treatment was evaluated in their work. Lo et al. [13] worked on ND:YAG laser hardening of martensitic stainless steel 440C and concluded that this process could be three times more successful than furnace heat treatment methods. Kim et al. [14] performed the surface hardening of carbon steel using ND:YAG laser. According to their work, increasing the power and scanning speed led to increase in the depth of hardness. Soriano et al. [15] measured the residual stress and mechanical properties of surface hardened austempered ductile iron and recommended the ND:YAG laser method for this material processing. Badkar et al. [16] studied the effects of process parameters in laser surface hardening of pure titanium using Nd:YAG laser. Li et al. [17] investigated the surface hardening process of AISI 1045 using high power diode and CO² laser. According to their work, performing the process using diode laser would result in higher quality than CO² one. Bien et al. [18] studied the surface treatment of C80U steel by CO² laser considering pulse change in designed time ranges. Telasang et al. [19] studied the wear and corrosion behavior of AISI H13 tools steel after performing surface hardening process. Pinahin et al. [20] presented the appropriate process for increasing wear resistance and mechanical behavior of several hard alloys using pulsed laser hardening. Babu et al. [21] investigated the effect of process parameters on microstructure and surface hardness of EN25 steel. They improved the surface hardness of the material two times more than base metal. Moradi et al. [22] presented a research paper in which the effect of laser pulse energy and focal point position on laser surface hardening of AISI 410 stainless steel was studied. Bojinovic et al. [23] simulated the laser hardening process and studied the temperature distribution on an austenitic stainless steel regarding the process parameters. Cordovilla et al. [24] analyzed the surface laser hardening of AISI 4140 steel using FEM. Their method was validated by performing experimental tests considering the process overlap tracks.

In the literature, the diode laser surface hardening of AISI 420 steel was not addressed before. In this work, the effect of laser process parameters like power, scanning speed and focal plane position have been studied in the

surface hardening process of AISI 420. The resulted hardened layer of pieces has been measured in depth and width and the microhardness has been evaluated in selected locations. Also the microstructure evolution have been studied after performing the process using optical microscope (OM) and FESEM.

2 Experimental Work

In the present work, AISI 420 martensitic stainless steel with the chemical composition as shown in Table 1 was studied as the work material. The disk shape samples with thickness of 10 mm and diameter of 75 mm were machined and grinded. Figure 1 shows the schematic of the laser surface hardening process.

In the experiments, a 1600 W diode laser was used for surface hardening of samples. Experimental settings and results of laser hardening process are shown in Table 2. As shown, the ranges of the input variables were: Laser power (1000–1600 W), scanning speed (5–7 mm/s) and focal plane position (60–75 mm).

Figure 2 shows the images of AISI 420 hardened samples. The numbers written on the samples in Fig. 2 are the test numbers from #1 to #7 according to Table 2. The hardened samples were cut in the middle of the process line. To prepare the metallurgical samples, cut specimens were mounted, polished and etched in the vilella's reagent (C6H3N3O7 2gr, Hcl 5 cc, C2H5OH 100 cc).

The cross section geometry (width and depth) of the hardened zone was measured using BUEHLER MET B7

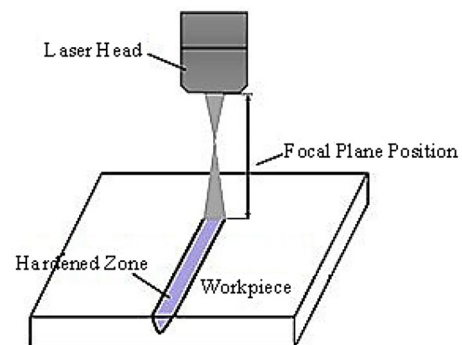


Fig. 1 Schematic of the laser surface hardening process

Table 1 Chemical composition of AISI 420 stainless steel (Wt.%)

Element name (Wt.%)	C	Si	Ni	Mn	P	S	Cr	Mo	Al	V	Fe
AISI 410 stainless steel	0.20	0.50	0.08	0.51	0.034	0.005	12.49	0.01	0.002	0.02	Balance

Table 2 Experimental settings and results

Test no	Input parameters			Output results		
	Scanning speed (mm/s)	Stand-off distance (mm)	Laser power (W)	Maximum hardness (HV)	Depth of hardness (mm)	Width of hardness (mm)
1	5	65	1400	720	1.2	6.1
2	5	75	1400	250	0.51	7.33
3	5	65	1000	478	0.77	6.7
4	7	65	1000	300	0.7	6.5
5	7	70	1600	375	1	6.2
6	6	70	1200	300	0.53	7.2
7	6	60	1200	800	1.3	5.1

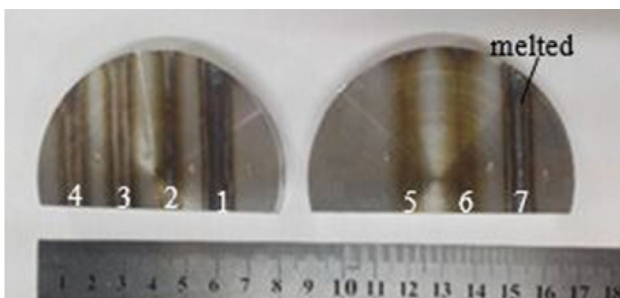


Fig. 2 Image of laser hardened samples for test conditions #1 to #7

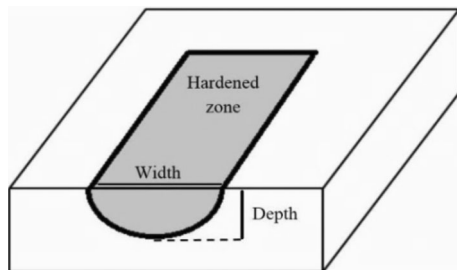


Fig. 3 Cross section of laser hardened zone

optical microscope and Image software. Figure 3 shows the schematic of hardened zone.

The microhardness was measured at least three times for each sample along the depth and width of laser affected zone of sample sections using a micro indentation tester (BUEHLER, USA). The hardness profiles in the laser affected zone along the depth and width directions were plotted for each sample and compared.

3 Results and Discussion

In this work, the effect of laser power, scanning speed and focal plane position in laser surface hardening of AISI 420 steel was studied. The studied results were dimensions of hardened layer, microhardness distribution in laser affected zone and hardened area microstructure.

3.1 Microhardness Distribution

In Fig. 4 the cut section of a sample is shown. For each sample, the microhardness was measured along the depth and width of hardened zone.

Heat input [9] in laser materials processing was used for better understanding of the process. It could be calculated using Eq. (1).

$$\text{Heat input} = \text{Laser power} / \text{Scanning Speed} \quad (1)$$

Therefore, by increasing the laser power and decreasing the scanning speed, heat input increases and more area of the material will be heated. For Figs. 5 and 6, by using this heat input equation, it is observed that sample #5 has 228.6 J/mm and sample #6 has 200 J/mm when the FPP is the same. Therefore it is obvious that when sample #5 has more heat input, the depth of hardness and maximum hardness will be more than sample #6 with lower heat input.

Figure 6 shows the distribution of microhardness over half the width along the cross section for samples #5 and #6 which have been processed by heat input 229 and 200 W/mm

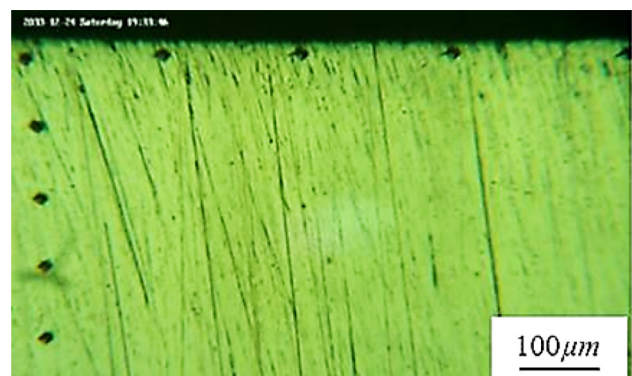


Fig. 4 Cross-sectional view of Vickers indenters along depth and surface of hardened zone

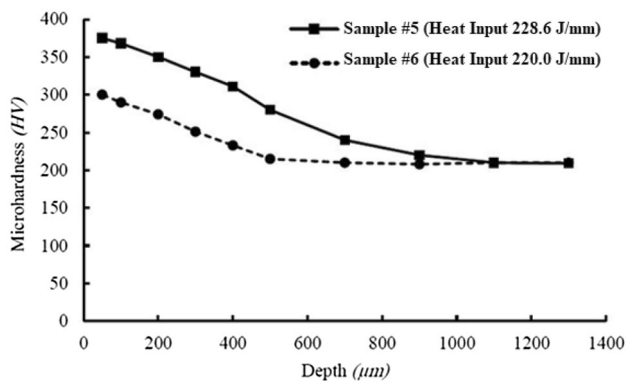


Fig. 5 Microhardness distribution profile along depth of the laser hardened layer (comparison of the heat input effect)

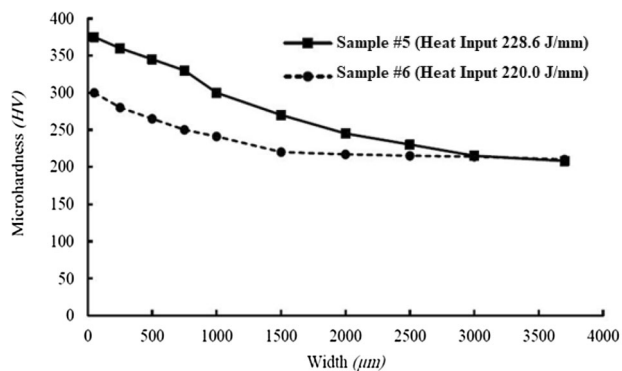


Fig. 6 Microhardness distribution profile along width of the laser hardened layer (comparison of the heat input effect)

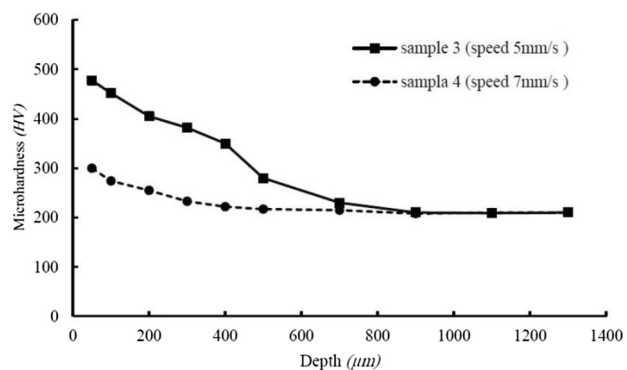


Fig. 7 Microhardness distribution profile along depth of the laser hardened layer (comparison of the scanning speed effect)

respectively. At the centerline of the sample, that is near to the laser beam, the microhardness is at its maximum value and gradually decreases departing from the centerline. It is crystal clear that the hardness distribution is like a sinusoidal function and the hardness is maximum in the center and decreases gradually along the outside of hardened zone. The reason of this phenomena is shape of the distribution of the

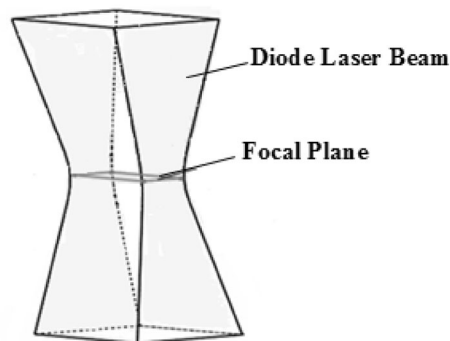


Fig. 8 Schematic of diode laser beam distribution

Table 3 The area of the laser beam interaction with the material

Focal plane position (mm)	Beam Area in interaction with material surface (mm ²)
60	12
65	25.34
70	42.77
75	64.3

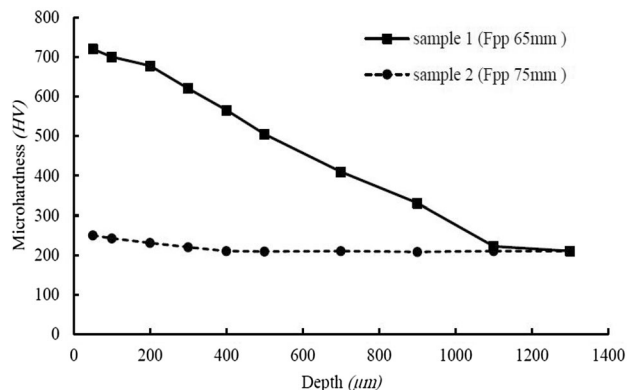


Fig. 9 Microhardness distribution profile along depth of the laser hardened layer (comparison of the focal plane position effect)

laser beam energy. As mentioned before, the microhardness value and width of sample #5 is more than sample #6 because of higher heat input.

According to this work, the scanning speed has a direct effect on the process results. By decreasing the scanning speed, the interaction time of the laser beam and heat input energy increases. So, the energy density become higher and the hardness value and its effect area enlarges. In Fig. 7, scanning speed of sample #3 is more than sample #4 and so the process is more effective in the former than the latter sample.

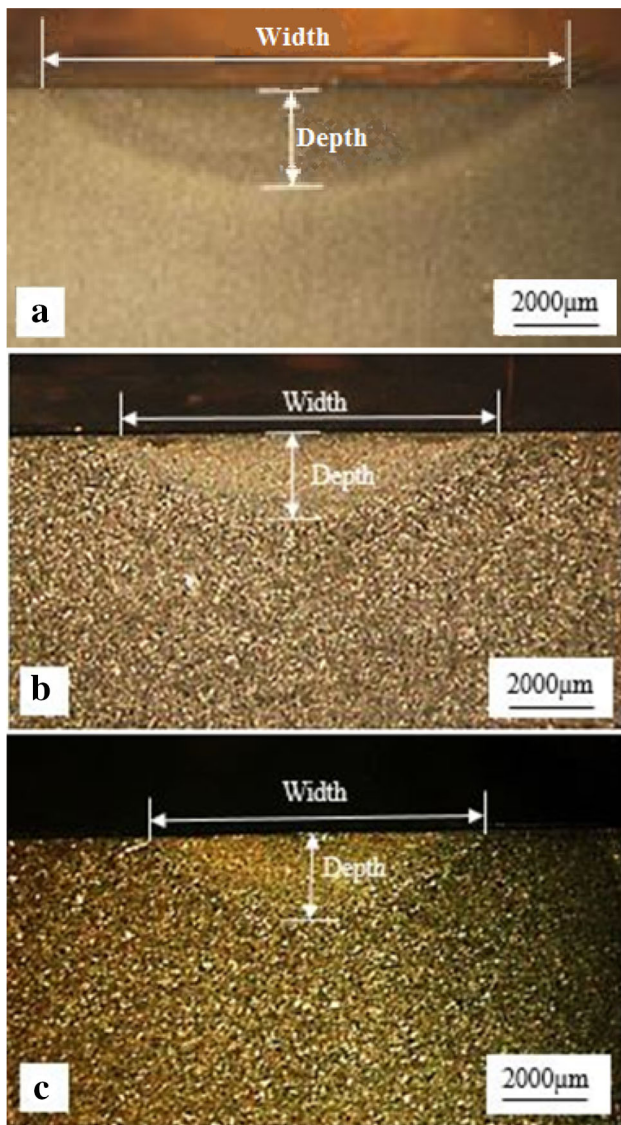


Fig. 10 Cross section of laser hardened samples **a** sample # 1, **b** sample # 3, **c** sample # 7

3.2 Geometrical Dimensions of Hardened Layer

Figure 8 displays the distribution of laser beam energy in the direction of its movement. As illustrated, the focal plane position affects the input energy concentration and geometrical dimension of processed area. Increasing the focal plane position leads to the divergence of the laser beam and decrease in the energy density while the beam area interaction with the material increases.

Focal plane position equal to 60 mm means that the focal plane is above the surface and in this case the red area will be 12 mm^2 (the dimension of the Focal Plane is $8 \times 1.5 \text{ mm}$). The material surface which the laser beam interact with is calculated. It may be mentioned that the divergence angle of the beam is different in two sides. In

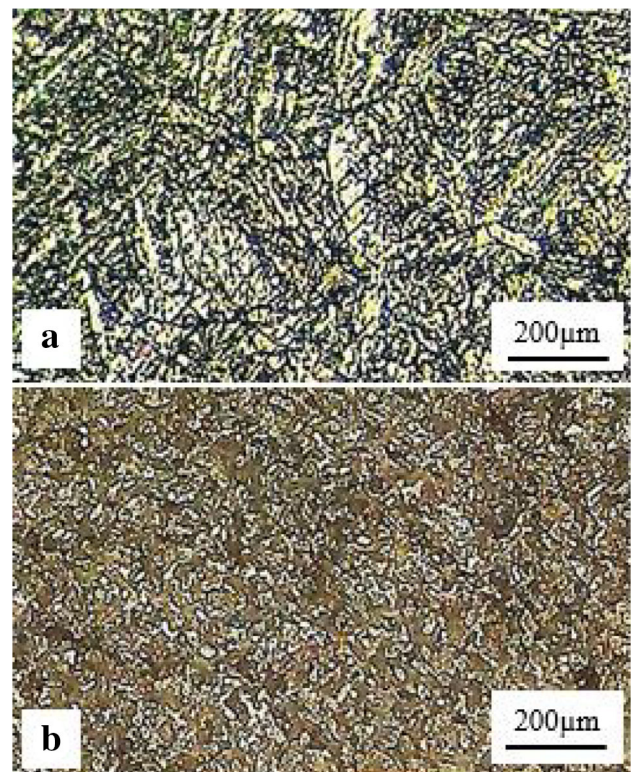


Fig. 11 **a** Microstructure of base martensitic stainless steel AISI 420, **b** microstructure of laser hardened metal sample #4

the Fast (1.5 mm) and Slow (8 mm) sides, the divergence angles are 11 and 6 degree, respectively (Table 3).

Figure 9 shows the microhardness value and its depth for samples #1 and #2 with 65 and 75 mm focal plane position respectively. As the focal plane position rises, the maximum hardness and penetration depth reduces but the affected width increases.

For measuring the geometrical dimensions of laser affected area, the macrographic examination of samples have been carried out which are shown in Fig. 10 for samples #1, #3 and #7 after grinding, polishing and etching procedure.

According to Table 2 and comparing samples #1 and #2, by increasing the focal plane position from 65 to 75 mm, the depth of hardened zone decreases while the width increases.

3.3 Microstructure of Hardened Layer

The microstructure of samples have been studied in this work via metallographic attempts and optical microscopy. Figure 11a illustrates the microstructure of material before laser processing. It is realized that some ferrite phase is distributed in the base martensitic field. Figure 11b shows the microstructure of laser processed sample #4 without any ferrite phase in the material.

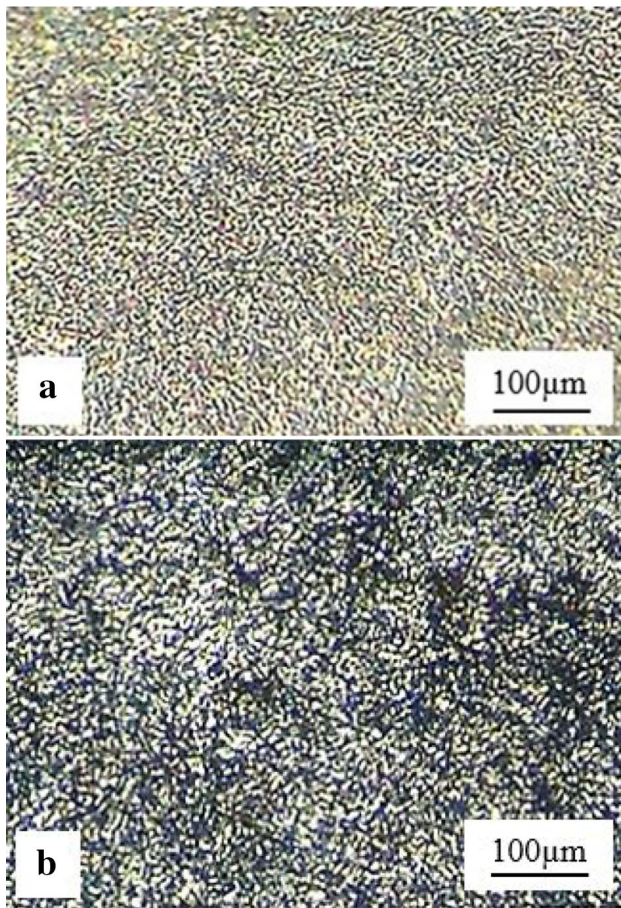


Fig. 12 Microstructure of laser hardened zone of martensitic steel AISI 420 **a** sample #1, **b** sample #2

Microstructure of processed samples #1 and #2 are shown in Fig. 12 which reveal the full martensitic phase in the microstructure. According to investigations, increasing the heat input energy in the process via using higher laser power, lower scanning speed and lower focal point position distance leads to increasing the austenite phase temperature and finally decreases the austenite grain sizes. Also it is evident that by controlling the scanning speed, the uniformity of grains can be achieved.

FESEM images of base material and laser hardened sample #1 are shown in Fig. 13. According to Fig. 13b, the carbide particles are made fine and are distributed in the structure while the ferrite phase dissolves and declines in size. In the microstructure of base metal (Fig. 13a), the laminated and spherical carbides exist in the grain boundaries and grains, respectively. In the laser processed material, the laminated carbides dissolve in the grain boundaries while spherical ones remain in the grains as shown in Fig. 13b.

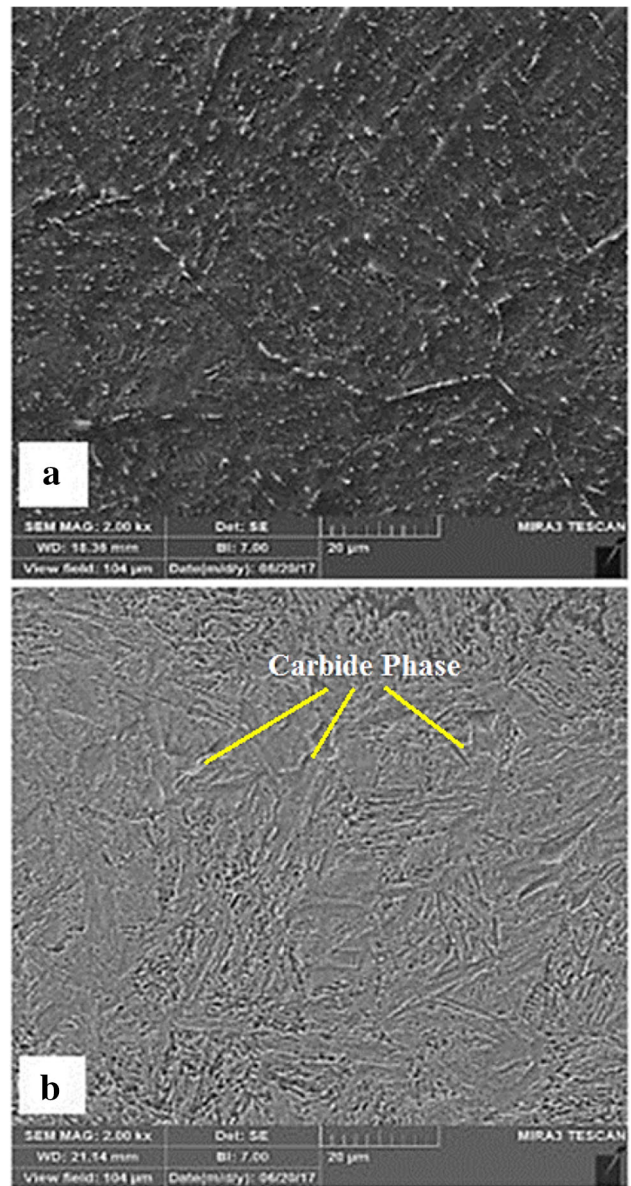


Fig. 13 FESEM image **a** base material of AISI 420, **b** laser hardened sample # 1

4 Furnace Hardening of AISI 420

For comparing the laser surface hardening method with conventional method, the furnace heat treatment according to cycle presented in Fig. 14 is conducted. The material is preheated to 540 °C for 1 h and heated to 980 °C at the rate of 70 °C/h and is kept at that temperature for 2 h. The sample is quenched in oil, water and air and the hardnesses are reported as 528, 560 and 513 Vickers, respectively.

Due to the possibility of micro-crack formation in the water, and lower hardness in air, the oil is an ideal quenching method with a hardness of 528 Vickers for AISI

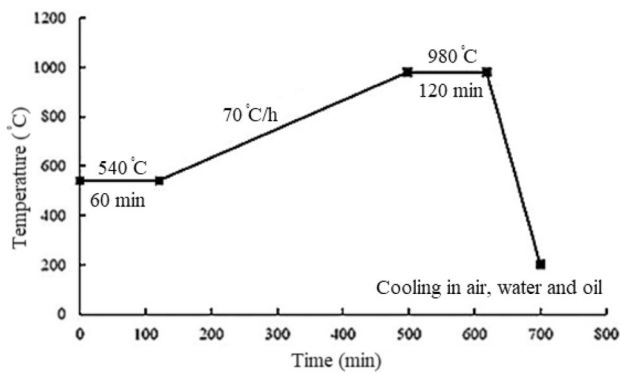


Fig. 14 furnace hardening heat treatment cycle of AISI 420 used in this research

Table 4 Comparison of furnace hardening heat treatment and laser hardening

Heat treatment cycle	Furnace hardening heat treatment (Vickers)	Laser hardening (Vickers)
Cooling in oil	528	–
Cooling in water	560	–
Cooling in ear	513	–
Laser surface hardening	–	800

420. So the hardness value with the diode laser hardening method (800 Vickers) is 1.5 times than the furnace hardening heat treatment. Table 4 shows the comparison of the hardness results of furnace hardening heat treatment and laser surface hardening.

The microstructure of furnace hardened sample is compared with laser processed sample in Fig. 15. The fine carbide particles in furnace processed sample dispersed in the martensitic field. In the laser processed sample, due to relatively high cooling rate, these particles are interconnected which causes reduction in strength and hardness of the material. For decreasing the ferrite field and to overcome the problem, higher laser power should be selected and scanning speed should be lower. Also due to high energy concentration, localized hardness occurs.

5 Conclusions

In this work, the effect of laser power, scanning speed and focal plane position have been investigated in diode laser surface hardening process of AISI 420. The studied outputs are geometrical dimensions of hardened layer (i.e. width and depth), microhardness values in laser affected area and samples microstructures. According to experimental works, the following results can be concluded:

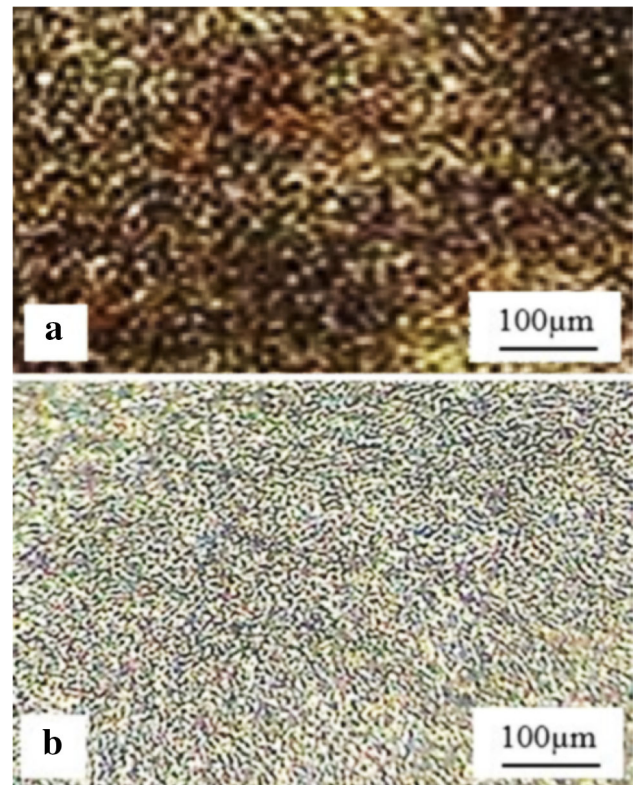


Fig. 15 a Microstructure of furnace hardening AISI 420, b microstructure of laser hardened sample #1

1. By increasing the laser power and decreasing the scanning speed, the heat input increases which leads to increase in the microhardness and geometry of the affected area.
2. Reducing the focal plane distance causes more energy density resulting in increase in the depth and microhardness of hardened layer.
3. Increase of microhardness from 210 to 720 HV with depth of 1.2 mm and width of 6.1 mm, is possible by using laser surface hardening process of AISI 420 stainless steel.
4. The value of the surface hardness in laser surface hardening process is about 25% more effective than conventional hardening process.
5. Laser surface processing of martensitic stainless steel AISI 420 causes change in initial ferrite phases of the base metal to completely martensitic phase. Also by controlling the process parameters, it is possible to control final product microstructure and uniformity of grains.

References

1. Kannatey Asibu E, Jr, *Principles of Laser Materials Processing*, John Wiley and Sons, New Jersey (2009), p 568.
2. Moradi M, Salimi N, Ghoreishi M, Abdollahi H, and Shamsborhan M, *J Laser Appl* **26** (2014) 022004.
3. Sundqvist J, Kaplan A F H, Granström J, and Sundin K G, *J Laser Appl* **27** (2015) 042002.
4. Moradi M, Ghoreishi M, Torkamany M, Sabbaghzadeh J, and Hamed MJ, *Adv Mat Res* **383** (2012) 6247.
5. Faraji A H, Moradi M, Goodarzi M, Colucci P, and Maletta C, *Opt Lasers Eng* **96** (2017) 1.
6. Khorram A, Jafari A, and Moradi M, *Modares Mech Eng* **17** (2017) 129.
7. Moradi M, Ghoreishi M, and Khorram A, *Laser Eng* **39** (2018) 379.
8. Moradi M, and Golchin E, *Lat Am J Solids Struct* **14** (2017) 464.
9. Moradi M, Mehrabi O, Azdast T, and Benyounis H Y, *Opt Laser Technol* **96** (2017) 208.
10. Li L, *Opt Lasers Eng* **34** (2000) 231.
11. Puli R, and Ram G D J, *Surf Coat Technol* **209** (2012) 1.
12. Mahmoudi B, Aghdam A R S, and Torkamany M J, *JEST* **8** (2010) 87.
13. Lo K H, Cheng F T, and Man H C, *Surf Coat Technol* **173** (2003) 96.
14. Kim J D, Lee M H, Lee S J, and Kang W J, *Trans Nonferr Metal Soc* **19** (2009) 941.
15. Soriano C, Leunda J, Lambarri J, Navas V G, and Sanz C, *Appl Surf Sci* **25** (2011) 7101.
16. Badkar D S, Pandey K S, and Buvanashakaran G, *T Nonferr Metal Soc* **20** (2010) 1078.
17. Li R, Jin Y, Li Z, and Qi K, *J Mater Eng Perform* **23** (2014) 3085.
18. Bien A, and Szkodo M, *J Mater Process Tech* **217** (2015) 114.
19. Telasang G, Majumdar J D, Padmanabham G, and Manna I, *Surf Coat Technol* **261** (2015) 69.
20. Pinahin I A, Chernigovskij V A, Bracihin A A, and Yagmurov M A, *J Frict Wear* **36** (2015) 330.
21. Babu P D, Buvanashakaran G, and Balasubramanian K R, *T Can Soc Mech Eng* **36** (2012) 241.
22. Moradi M, Karami Moghadam M, Zarei J, and Ganji B, *Modares Mech Eng* **17** (2017) 311.
23. Bojinovic M, Mole N, and Stok B, *Surf Coat Technol* **273** (2015) 60.
24. Cordovilla F, Garcia-Beltran A, Sancho P, Dominguez J, de-Lara L R, and Ocana J L, *Mater Des* **102** (2016) 225.